

Z-PINCH RESEARCH ON THE 20-MA Z ACCELERATOR *

C. A. Coverdale, B. Jones[#], C. Deeney, D. J. Ampleford, J. E. Bailey, D. E. Bliss, M. E. Cuneo, C. J. Garasi, S. V. Lebedev[†], P. D. LePell[‡], D. H. McDaniel, T. A. Mehlhorn, J. L. Porter, C. L. Ruiz, and D. B. Sinars

Sandia National Laboratories, PO Box 5800, Albuquerque, NM 87185 USA

[†]Blackett Laboratory, Imperial College, London, SW7 2BZ, UK

[‡]Ktech Corp., Albuquerque, NM 87123 USA

Abstract

Z-pinch sources have been studied at the Z accelerator with a wide variety of load configurations; applications include inertial confinement fusion and K-shell x-ray emission. Underlying physics issues for these experiments are related; understanding the ablation, implosion, and stagnation physics aids in optimization of wire array loads for radiation power production. Experiments have been fielded to study these z-pinch phases, for the various applications, with a goal of optimization of the radiated output. Studies of ablation and implosion with x-ray backlighting, and insight into stagnation physics through self-emission imaging and spectroscopy, have provided valuable information on the dominant physical processes governing z pinch radiation sources. The evolution of instability growth has also been studied.

INTRODUCTION

The Z Accelerator [1] can provide up to 20 MA in 100 ns to an imploding load and has been demonstrated to be the brightest laboratory x-ray source, with > 1.8 MJ radiated output and > 250 TW radiated power [2]. Pulsed power is also an efficient source of radiation, with a conversion efficiency of $\sim 15\%$ from wall plug electrical input to x-ray output. Research over the last several years utilizing this capability has focused on basic z-pinch physics research [3,4], inertial confinement fusion (ICF) [5,6,7] and K-shell x-ray sources [8,9,10]. These research areas are intertwined by the basic physics associated with z pinches, from the earliest stage of wire initiation to the later stages of ablation, implosion, stagnation and disruption. Diagnostic advances in the last few years, including x-ray backlighting [11] and monochromatic self-emission imaging [12] have allowed for detailed study of ablation, implosion, and stagnation physics.

Challenges for ICF and K-shell sources alike include optimization of the z-pinch output for the specific application and understanding the dominant physics that restricts this output. In these Proceedings, highlights of research that has been performed by Sandia National Laboratories is presented. Basic physics research on the evolution of wire array z pinches, ICF studies, and K-

shell x-ray sources will be discussed, with an emphasis on the understanding of z-pinch plasma physics.

BASIC Z-PINCH PHYSICS STUDIES

Wire array z-pinch dynamics can be heuristically divided into five stages: wire initiation, ablation, implosion, pinch stagnation, and disruption. These phases of the plasma evolution have been investigated at lower current [13,14], and also observed at 14-20 MA on the Z machine [15,16]. Figure 1 shows 1.865 keV radiography from 20-mm-diameter, 300-wire tungsten arrays on Z, and corresponding timing of these frames (A-D) relative to the current pulse, calculated zero-dimensional (0D) thin-shell trajectory, and total x-ray power pulse. Wire initiation and expansion (A) is accompanied by the formation of low-density coronal plasma surrounding a dense wire core [17]. In the ablation stage (B), the wire core is ablated, with low-density material streaming to the array axis and pre-filling the volume interior to the array. Non-uniform wire ablation [17,18] seeds magnetic Rayleigh-Taylor (MRT) instabilities that grow during the array implosion (C), which results in fingers of mass trailing the main implosion (D) and three-dimensional (3D) structure during the array stagnation [19]. In the disruption phase, x rays are emitted at lower power than during stagnation as $m=0$ and $m=1$ magnetohydrodynamic (MHD) instabilities grow, ultimately breaking apart the plasma column and terminating x-ray production.

MRT-type implosion instabilities observed in wire array

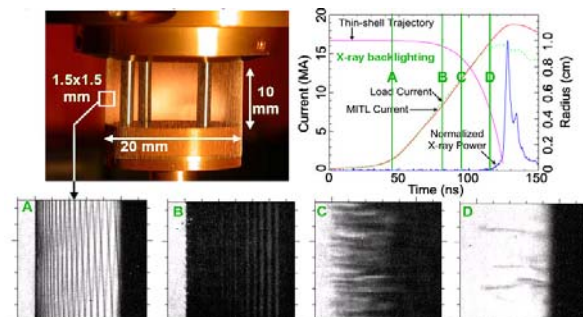


Figure 1: Example radiography data from 300-wire, 6-mg tungsten arrays on Z illustrating several stages of z-pinch implosions. Excerpted from D. B. Sinars *et al.*, Physics of Plasmas, **12**, 056303 (2005), Copyright 2005, American Institute of Physics.

* Sandia is a multiprogram laboratory operated by Sandia Corporation, a Lockheed Martin Company, for the United States Department of Energy under contract DE-AC04-94AL85000.

[#]cacover@sandia.gov; bmjones@sandia.gov

z pinches are important in determining the resulting x-ray pulse width, as they lead to a distributed arrival of mass on the array axis during stagnation. They also produce trailing mass that may shunt current from the main implosion. To further study the evolution of non-linear MRT instability, experiments have been fielded with controlled seeding of initial perturbations in the wires. Modulations in wire radius were chemically etched into 15- μm -diameter Al 5056 at Sandia [20], and then fielded in 8- or 16-wire z -pinch experiments on the 1 MA MAGPIE generator at Imperial College [21,22]. As seen in Fig. 2, imploding bubbles were observed to form early in time at points of discontinuity in wire radius. The start of the main x-ray power rise occurred when these bubbles reached the array axis [22] and formed a dense, stagnated pinch with trailing remnants of the seeded bubbles (Fig. 2).

This behavior is consistent with 3D MHD simulation of one period of wire modulation performed with Sandia's ALEGRA-HEDP code [23], also shown in Fig. 2. The seeded perturbation in wire cores is imprinted on the coronal plasma and thus on the path of current in the corona. Local magnetic field enhancements occur near discontinuities in the current path, enhancing $|\mathbf{j} \times \mathbf{B}|$ and the mass ablation rate, depleting the wire core and initiating imploding bubbles while the surrounding wire sections are still ablating. The current-carrying bubbles implode toward the axis, leaving regions of trailing mass as seen in the experimental data. While these studies involved controlled perturbations, the same basic instability dynamics likely applies to standard wire arrays in which $m=0$ coronal plasma structures [17] perturb the current path and seed MRT-type instabilities. Likewise, the growth of imploding bubbles and their role in delivering mass and energy to the stagnated plasma column has been studied in standard wire arrays [24].

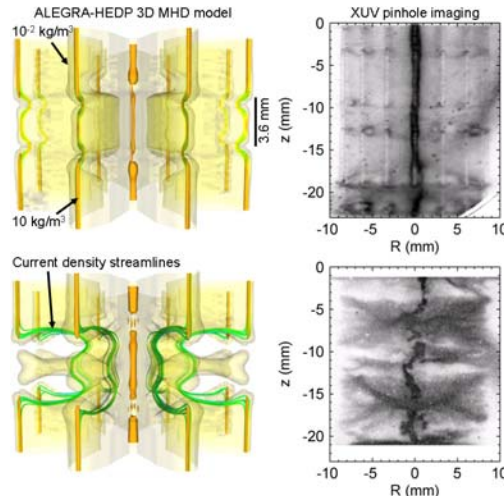


Figure 2: Simulated and experimentally observed evolution of wire array instabilities with seeded initial perturbations. Excerpted from B. Jones *et al.*, Physics of Plasmas, **13**, 056313 (2006), Copyright 2006, American Institute of Physics.

At stagnation, the imploding material assembles on axis into a high-energy-density column. The plasma carries with it significant implosion kinetic energy, and compressional $p \, dV$ work and Ohmic heating can also contribute significantly during this stage [19]. Other plasma heating mechanisms including anomalous resistivity [25], magnetic field dissipation [26], and ion viscosity [27] have also been proposed, the latter also offering an explanation for the high and persistent ion temperatures (>200 keV for stainless steel) observed on Z. (These mechanisms may play a significant role in the plasma energy balance during the disruption phase following peak x-ray power.) The dense stagnated plasma is highly collisional, and thus the energy input into the z pinch by $\mathbf{j} \times \mathbf{B}$ work during the implosion is quickly thermalized to the electrons and radiated as soft x-rays with pulse widths as short as a few nanoseconds on Z. The character of the stagnated z pinch will be discussed further in the section on K-shell radiators below, as those loads in particular provide an opportunity to study plasma conditions through x-ray spectroscopy.

Z-PINCH-DRIVEN INERTIAL CONFINEMENT FUSION

The high efficiency of soft x-ray generation with pulsed power makes this an attractive technology for inertial confinement fusion (ICF) studies, with the eventual goal of supporting a high-yield facility [5]. Sandia pursues a vigorous program in z -pinch-driven ICF on the Z machine, and the following briefly describes two concepts for indirect drive capsule implosion using z -pinch radiation sources.

Double-ended z -pinch vacuum hohlraum

The double-ended hohlraum (DEH) concept, proposed in Ref. [28] and illustrated in Fig. 3, uses two high-current wire array z pinches (top pinch TP and bottom pinch BP) to drive a secondary hohlraum (SH) containing an ICF capsule. This approach decouples the physics of capsule implosion from z -pinch x-ray generation to a degree, and provides control of capsule symmetry through tuning of the SH geometry [29].

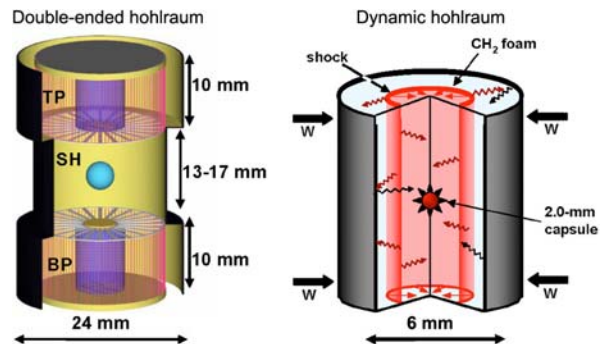


Figure 3: Two z -pinch-driven ICF concepts investigated on Sandia's Z machine. Excerpted from M. K. Matzen *et al.*, Physics of Plasmas, **12**, 055503 (2005), Copyright 2005, American Institute of Physics.

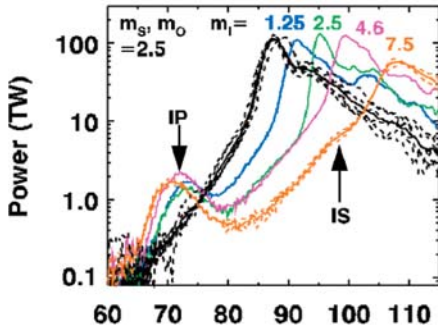


Figure 4: X-ray pulse shape control for ICF studies on Z using nested tungsten wire arrays with variable inner array mass. Reprinted with permission from M. E. Cuneo *et al.*, Phys. Rev. Lett. **95**, 185001 (2005). Copyright 2005 by the American Physical Society

Significant progress has been made on Sandia's Z machine in understanding the dynamics of compact 20-mm-diameter tungsten wire arrays used in DEH studies; Ref. [6] presents a detailed overview of this work. The evolution of such a load, as shown in Fig. 1, was discussed in the previous section. Soft x-ray yields of 1.0-1.8 MJ are produced on Z with compact z pinches, with up to 1 MJ of this energy useful for ICF capsule drive.

The need to tailor the radiation pulse shape to provide an appropriate capsule drive history is generic to all indirect drive schemes [30], and requirements for the DEH are discussed in Ref. [28]. Nested wire arrays have previously been demonstrated to narrow the main x-ray pulse and increase the peak radiated power on Z [2] and have more recently been shown to provide controlled x-ray pulse shaping for ICF applications [31]. Figure 4 shows x-ray pulses produced with a 20-mm-diameter tungsten outer array with mass $m_o=2.5$ mg, and a second inner array with 12 mm diameter and variable mass m_i . The three shocks necessary to drive the capsule on a low adiabat [6] are provided by the interaction pulse (IP) produced when the imploding outer array encounters the inner array, the inner strike (IS) when material from the inner array arrives on axis, and the main x-ray pulse at final stagnation. The timing of these pulses can be controlled through design of the wire array geometry, *i.e.* by choosing the appropriate m_i .

Z-pinch dynamic hohlraum

Another concept for z-pinch ICF pursued on Z is the dynamic hohlraum (DH), shown schematically in Fig. 3 and described in detail in Ref. [7]. A nested 40-mm- on 20-mm-diameter tungsten wire array implodes onto a foam column, driving a cylindrically converging shock which acts as a radiation source to drive an ICF capsule at the center of the foam. The tungsten plasma from the imploded wire array surrounds the foam and acts as a hohlraum, trapping the radiation from the shock. This concept involves closer coupling of z-pinch and capsule

dynamics, produces a greater challenge for capsule symmetry control, but also provides greater drive efficiency.

Experiments on the Z machine have produced $>2 \times 10^{11}$ thermonuclear DD neutrons through DH-driven 2-mm-diameter capsule implosion [7,32]. The dense implosion cores produced with this efficient drive configuration have been studied through gated x-ray spectroscopy, spatially-resolved from multiple simultaneous viewing directions [33]. An argon dopant in the capsule fuel emits K-shell lines whose analysis indicates ~ 1 keV electron temperatures and $1-4 \times 10^{23} \text{ cm}^{-3}$ electron densities in the prolate imploded capsule. The measured capsule asymmetry is consistent with two-dimensional modeling in this case where no techniques have been employed to improve capsule drive uniformity.

K-SHELL SOFT X RAY GENERATION

The generation of K-shell x-rays necessitates different load conditions than that which is desirable for the ICF work. In order to achieve the high electron temperatures (>2 keV) and ion densities ($>10^{18} \text{ cm}^{-3}$) necessary to produce significant K-shell output, large diameter loads ($>40\text{mm}$) are necessary [34]. The thermal energy of the ions is the primary source of heating for the electrons, through rapid conversion of this energy to heat at stagnation. Large diameter loads lead to high implosion velocities, and therefore higher kinetic energy per ion. The ion temperature can continue to increase in the adiabatic compression, or through ion viscous heating [27], that follows stagnation, as evidenced by the high ion temperatures measured in the K-shell sources. As the K-shell photon energy increases, the initial load diameter necessary to achieve appropriate temperatures and densities increases, as detailed in Ref. [34] and [35]. The temperature and density can be inferred from experimental measurements of the K-shell spectrum, and compared with estimates from theory and simulation, offering insight into the stagnated plasma that is not possible with present high-atomic-number wire array configurations.

Experiments over the last several years at Z have evaluated a variety of K-shell sources, from aluminum at 1.8 keV up to copper at 8.4 keV photon energy [8,9,10]. Plotted in Fig. 5 are the results of experiments designed to study the K-shell output from stainless steel wire arrays. Stainless steel, which is comprised primarily of chromium, iron, and nickel, radiates in the K-shell from 5.5 to 7.8 keV. The 0D calculated implosion velocity was determined from modeling with the Scream code. As seen in Fig. 5, the single wire arrays radiate more than an equivalent nested array. However, single array K-shell output is dominated by isolated regions of high temperature and density which result from the growth of instabilities, particularly MRT [36]. Large diameter arrays, either single or nested, are particularly susceptible to the growth of MRT. As mentioned earlier, nested wire arrays have been shown to increase the radiated power

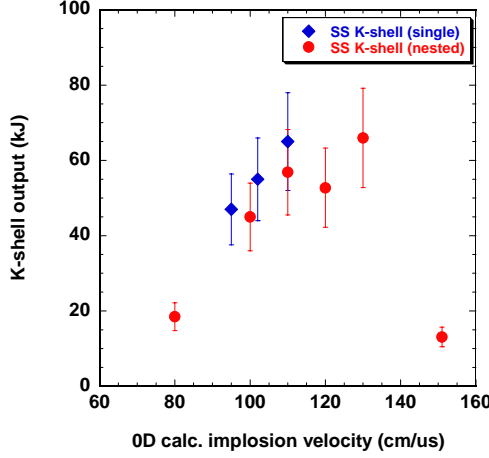


Figure 5: Comparison of 5.5 – 8.5 keV x-ray emission from single and nested stainless steel wire arrays.

through improvements in the x-ray pulsedshape [2]. This same effect is observed with the K-shell-radiating wire arrays. Additionally, the nested arrays have been observed to have better axial uniformity in the K-shell, as well as faster risetimes and more reproducible radiated output, results consistent with a reduction in MRT.

No difference is observed between single and nested wire arrays for total radiated output. For most of the K-shell sources, the total radiated output is 1.2 – 1.3 MJ; the total radiated power follows the same trend as the K-shell. Since the nested arrays produce faster, narrower x-ray pulses than single arrays for K-shell emission and the more abundant soft x rays (<1 keV), higher K-shell power and higher total power are observed. Up to one-third the radiated energy is radiated after stagnation for these sources.

The inferred electron temperature from time-integrated spectra for a typical SS nested array is ~3.5 keV, with an ion density of $\sim 1.5 \times 10^{20} \text{ cm}^{-3}$. These values are inferred through comparison of measured line ratios with detailed collisional-radiative-equilibrium calculations of the line ratios [37]. For comparison, similarly optimized configurations for argon (3 keV photons) and titanium (4.7 keV photons) show ~2.4 keV [9] and ~3 keV [8] electron temperatures, respectively.

The development of an imaging system [38] that allows for monochromatic imaging of the pinch near stagnation has been helpful in understanding stagnation physics. The monochromatic image at 277 eV in Figure 6 shows significant structure before the peak radiated output, which, while evolving into a relatively stable pinch of narrower diameter after peak radiation, still contains noticeable features. The structure is indicative of instability growth (MRT) during the implosion, similar to that described earlier. At similar times, the K-shell radiation is emanating from a narrower, yet still structurally complicated, column on the axis. Given that

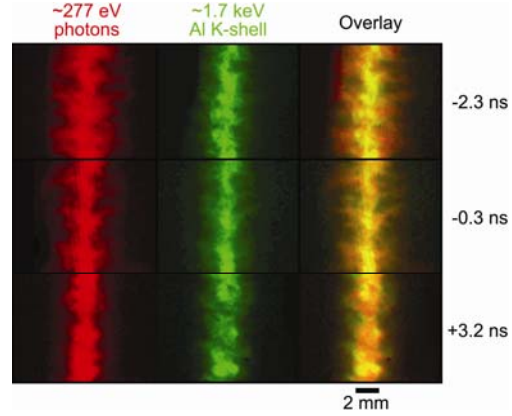


Figure 6: False color, 1-ns-gated images showing monochromatc ~277 eV photons and K-shell emission from an Al wire array on Z. Reprinted with permission from paper number 050692RSI, accepted for publication in Review of Scientific Instruments [38]. Copyright 2006, American Institute of Physics.

the plasma conditions necessary for the K-shell emission dictate high temperatures and densities, these images are evidence of a hot, dense region on the axis present both before and after stagnation, surrounded by a cooler blanket of material that is still imploding past the peak radiated output. The material that continues to implode is likely the trailing mass, as described earlier, and is cold and dense enough to be opaque to the K-shell, as evidenced in the +3.2 ns image of Fig. 6. This effect highlights the role of opacity for the lower atomic number K-shell radiators and the interplay between radiation transport and the 3D structure of the z pinch. If this opaque blanket can be disrupted, through a natural or seeded instability for example, more of the K-shell radiation could escape.

Similar images from this diagnostic for the K-shell sources have demonstrated that structure observed varies with atomic number, primarily in the K-shell emission. Specifically, for higher atomic number materials such as copper, the K-shell region is more localized. Again, this is indicative of the different plasma conditions necessary for the K-shell output with different atomic number, and highlights the difficulty in achieving these conditions for higher photon energies.

SUMMARY

To summarize, the Z Accelerator is capable of delivering up to 20 MA in 100 ns to imploding loads. Research at this facility covers a broad range of topics, from basic plasma physics to applications such as ICF and K-shell sources. Experiments studying the initial ablation and implosion phases of wire arrays have shown the growth of instabilities, which are further studied in a controlled manner with a seeded perturbation.

Inertial confinement fusion research on the Z machine encompasses several concepts for z-pinch-driven indirect capsule drive, two of which were discussed here. The double-ended hohlraum provides detailed control of capsule symmetry and decouples the physics between the ICF capsule and the z-pinch radiation source, making it simpler to address the scaling of the technique to higher current. The dynamic hohlraum provides closer coupling between z-pinch and capsule dynamics, allowing for greater drive efficiency and producing $>2 \times 10^{11}$ DD neutrons in Z capsule implosion experiments. Z-pinch dynamics have been extensively studied for compact ICF-relevant wire arrays, and the same basic physics governing evolution of the imploding plasma is relevant also for K-shell-radiating loads.

K-shell output up to 8 keV photon energy has been demonstrated at Z. Variations on load configurations for stainless steel wire arrays has shown that single arrays, which are dominated by hot spots, can produce more K-shell radiation than nested arrays, but with lower power due to the presence of instabilities. Electron temperatures and ion densities inferred from K-shell spectra verify that high temperatures and densities, necessary for K-shell emission, are obtained. Monochromatic imaging of the various K-shell sources has supported the study of stagnation physics. Hot, dense regions radiating in the K-shell have been observed, with a cooler blanket of material surrounding the primary K-shell emitting region.

Future work will focus on the assessment of z pinches at ZR, the 26 MA refurbishment of Sandia's Z machine anticipated to be completed in 2007.

REFERENCES

- [1] R.B. Spielman *et al.*, Phys. Plasmas 5 (1998) 2105.
- [2] C. Deeney *et al.*, Phys. Rev. Lett. 81 (1998) 4883.
- [3] J.E. Bailey *et al.*, Phys. Plasmas 9 (2002) 2186.
- [4] T.J. Nash *et al.*, Phys. Plasmas 11 (2004) L65.
- [5] M.K. Matzen *et al.*, Phys. Plasmas 12 (2005) 055503.
- [6] M.E. Cuneo *et al.*, Phys. Plasmas 13 (2006) 056318.
- [7] J.E. Bailey *et al.*, Phys. Plasmas 13 (2006) 056301.
- [8] C. Deeney *et al.*, Phys. Plasmas 6 (1999) 2081.
- [9] H. Sze *et al.*, Phys. Plasmas 8 (2001) 3135.
- [10] B. Jones *et al.*, J. Quant. Spectrosc. Radiat. Transfer 99 (2006) 341.
- [11] D.B. Sinars *et al.*, Phys. Plasmas 12 (2005) 056303.
- [12] B. Jones *et al.*, IEEE T. Plasma Sci. 34 (2006) 213.
- [13] S.V. Lebedev *et al.*, Plasma Phys. Control. Fusion 47 (2005) A91.
- [14] V.V. Aleksandrov *et al.*, Plasma Phys. Rep. 27 (2001) 89.
- [15] D.B. Sinars *et al.*, Phys. Rev. Lett. 93 (2004) 145002.
- [16] D.B. Sinars *et al.*, Phys. Plasmas 12 (2005) 056303.
- [17] S.V. Lebedev *et al.*, Phys. Rev. Lett. 85 (2000) 98.
- [18] C.J. Garasi *et al.*, Phys. Plasmas 11 (2004) 2729.
- [19] J.P. Chittenden *et al.*, Plasma Phys. Control. Fusion 46 (2004) B457.
- [20] B. Jones *et al.*, Rev. Sci. Instrum. 75 (2004) 5030.
- [21] B. Jones *et al.*, Phys. Rev. Lett. 95 (2005) 225001.
- [22] B. Jones *et al.*, Phys. Plasmas 13 (2006) 056313.
- [23] A.C. Robinson and C.J. Garasi, Comput. Phys. Commun. 164 (2004) 408
- [24] V.V. Ivanov *et al.*, accepted to Phys. Rev. Lett., (2006).
- [25] K.G. Whitney *et al.*, Phys. Plasmas 11 (2004) 3700.
- [26] L.I. Rudakov *et al.*, Phys. Rev. Lett., 84 (2000) 3326.
- [27] M.G. Haines *et al.*, Phys. Rev. Lett., 96 (2006) 075003.
- [28] J.H. Hammer *et al.*, Phys. Plasmas 6 (1999) 2129.
- [29] R.A. Vesey *et al.*, Phys. Rev. Lett. 90 (2003) 035005.
- [30] J.D. Lindl, Phys. Plasmas 2 (1995) 3933.
- [31] M.E. Cuneo *et al.*, Phys. Rev. Lett. 94 (2005) 225003.
- [32] C.L. Ruiz *et al.*, Phys. Rev. Lett. 93 (2004) 015001.
- [33] J.E. Bailey *et al.*, Phys. Rev. Lett. 92 (2004) 085002.
- [34] K.G. Whitney *et al.*, Phys. Rev. E 50 (1994) 2166.
- [35] J.W. Thornhill *et al.*, Phys. Plasmas 1 (1994) 321.
- [36] C.A. Coverdale *et al.*, submitted to IEEE T. Plasma Sci. (2006).
- [37] J.P. Apruzese *et al.*, J. Quant. Spectrosc. Radiat. Transfer 57 (1997) 41.
- [38] B. Jones *et al.*, accepted to Rev. Sci. Instrum. (2006)